X-/Ka-Band Dichroic Plate Design and Grating Lobe Study

J. C. Chen
Ground Antennas and Facilities Engineering Section

An X-/Ka-band dichroic plate is needed for simultaneously receiving X-band and Ka-band in the DSS-13 Beam Waveguide Antenna. The plate is transparent to the allocated Ka-band downlink (31.8–32.3 GHz) and the frequency band for the Mars Observer Ka-band Beacon Link Experiment (KABLE) (33.6–33.8 GHz), while at the same time reflecting the X-band downlink (8.4–8.5 GHz). The design is made using a computer program for dichroic plates with rectangular holes. The theoretical performance of the X-/Ka-band dichroic plate is presented. A study of the grating lobe problem is also included in this article.

I. Introduction

The bandwidth requirement for the X-/Ka-band dichroic plate at DSS 13 is 6.1 percent at Ka-band (31.8–33.8 GHz), whereas the desired bandwidth is 8.72 percent, which includes the Ka-band uplink (34.2–34.7 GHz). The holes on the dichroic plate have to be big enough for the low-frequency end of the Ka-band, but packed tight enough to prevent grating lobes at the high-frequency end. The wider the bandwidth, the more severe the grating lobe problem becomes. Also, there is a mechanical constraint for the wall thickness to ensure that the plate can support itself. There are over 10,000 holes for a 28-inch-diameter circular X-/Ka-band dichroic plate.

II. X-/Ka-band Dichroic Plate Design

The initial dimensions of an X-/Ka-band dichroic plate are scaled from the test S-/X-band dichroic plate, which is used to verify the computer code [1]. The reflection losses of the two orthogonal linear polarizations (TE and TM linear polarization) are not optimized in the test plate. Therefore, the cell size, the hole size, and the thickness of this plate are adjusted to meet the requirement, which is $\leq$ 0.2-dB reflection loss at the Ka-band Beacon Link Experiment (KABLE) frequency. The angle of incidence is $\theta = 30.0$ deg, $\phi = 0.0$ deg. The TE polarization is affected more by the changes of the X components of cell size and hole size than by the changes of Y components, while the TM polarization is affected more by the changes of the Y components of cell size and hole size than by the changes of X components for the angle of incidence $\phi = 0.0$ deg. The wall thickness is limited to a 0.008-in. minimum due to mechanical constraints.

The optimized design of the X-/Ka-band dichroic plate employs a rectangular hole of size 0.200 in. (H_x) by 0.203 in. (H_y); cell size 0.244 in. (D_x) by 0.211 in. (D_y) with a skew angle $\Omega = 60.0$ deg; and plate thickness (t) = 0.365 in. (Fig. 1). The amplitude and phase of the transmission and reflection coefficients are shown in Figs. 2–5. Reflection loss (transmission coefficient, dB) is less than 0.003 dB at the Ka-band downlink, 0.2 dB at the KABLE frequency, and 0.17 dB at the Ka-band uplink for both the

TE and TM linear polarizations. Since the received wave is circularly polarized, the reflection loss of the circular polarized wave at the KABLE frequency is around 0.1 dB, which meets the requirement. The phase shift between two linear polarizations is 3.4 deg to 4.0 deg at the Ka-band downlink, −0.2 deg to 0.5 deg at the KABLE frequency, and 1.8 deg to 3.8 deg at the Ka-band uplink (Fig. 6).

The tolerance of all the dimensions is 0.001 inch. Table 1 indicates the sensitivity of the reflection loss with respect to the hole size, which is the least controllable factor. The conductivity loss of the TE_{10} waveguide mode is 0.013 dB at the Ka-band downlink, 0.01 dB at the KABLE frequency, and 0.009 dB at the Ka-band uplink for a waveguide of size 0.203 in. by 0.200 in., thickness 0.365 in., and conductivity of copper 5.8×10^7 mhos/m [2].

III. Grating Lobe Study

Generally, the angle of transmission is equal to the angle of incidence (principal direction). But for certain circumstances, higher order modes are excited and some of the transmitted power leaves at an angle other than the principal direction. These excited higher order modes are called grating lobes and are similar to the grating lobes in phased array antennas. The conditions of the existence of a grating lobe depend on the angle of incidence, the frequency, and the size and skew angle of the cells on the plate. Since the incident wave is a horn pattern rather than a perfect plane wave, grating lobes may be generated by portions of the horn radiation that strike the plate at large angles of incidence.

The study of the grating lobe effects on a dichroic plate/feedhorn system is carried out in a series of steps. First, grating lobes that may be excited by a plane wave illumination are discussed. Next, expansion of a feedhorn pattern in terms of a group of plane waves traveling at different angles is described. Finally, the grating lobes that are excited by a horn pattern are determined.

A. Structure Dependence

For a certain angle of incidence ϕ, as θ is increased beyond some critical value ($\geq \theta_g$), grating lobes may be excited. Figures 7–9 show θ_g versus ϕ for different frequencies and cell sizes. The X-axis and Y-axis represent the angles ϕ and θ, respectively. For example, the point (0,55) in Fig. 7 indicates that when $\phi = 0.0$ deg, grating lobes are generated for $\theta \geq 55.0$ deg for the given cell size with respect to the wavelength. The θ_g curve changes when the skew angle of the cell changes (Fig. 7). Also, the higher the frequency, the smaller the θ_g for a given cell size. Figure 8 shows the θ_g curve for wavelength 1.2 D to 1.6 D on a cell of $D_x = D, D_y = 0.866\ D$, and $\Omega = 60$ deg, where D is a unit length. Figure 9 shows how the sizes of cells affect the value of θ_g.

B. Horn Pattern Expansion

The far-field horn pattern can be represented as a plane wave expansion, i.e., a group of plane waves traveling with different amplitudes at different angles. If the horn is placed at θ_0, ϕ_0, the different angles of incidence of these plane waves on the dichroic plate may be calculated through a coordinate transformation from the horn coordinate system to the dichroic-plate coordinate system. The far-field horn pattern is assumed to be symmetric in ϕ. Figures 10 and 11 show the angle of incidence on a dichroic plate from a horn with a symmetric pattern placed at $\theta_0 = 15.0$ deg, $\phi_0 = 0.0$ deg, and $\theta_0 = 30.0$ deg, $\phi_0 = 0.0$ deg, respectively. Each curve is for a constant θ_h in the horn coordinate system. For a 22-dB horn, $\theta_h = 12.0$ deg is about −12 dB with respect to the on-axis peak and $\theta_h = 14.0$ deg is about −14 dB.

C. Excitation of Grating Lobes by Horn Patterns

The grating lobe plot and the horn pattern plot need to be overlapped to determine the severity of the grating lobe problem for a given horn/dichroic plate geometry. For example, from the test S-/X-band dichroic plate experiment, the discrepancies between the calculation and measurement start above 8.6 GHz for TM polarization (Fig. 12) [1]. The conditions of the experiment are depicted in Fig. 13. The principal direction of the radiation from the 22-dB X-band horn strikes the plate at an angle of $\theta_0 = 30.0$ deg, $\phi_0 = 90.0$ deg. For 8.6 GHz, the θ_g curve intersects the $\theta_h = 14.0$ deg contour of the horn pattern, which corresponds to −14 dB with respect to the center radiation. Therefore, the disagreement between theory and experiment can be attributed to grating lobes excited by horn radiation that are at least 14 dB below the peak. Furthermore, Fig. 13 indicates that the grating lobe problem would be less severe if the principal direction of the horn was shifted to $\phi_0 = 0.0$ deg for $\theta_0 = 30.0$ deg.

For the X-/Ka-band dichroic plate, the horn is tilted 30 deg from normal at $\phi = 0.0$ deg (Fig. 14). The θ_g curve for 33.8 GHz (the high end of the KABLE frequency band) intersects with $\theta_h > 16.0$ deg curves, which is equivalent to 16 dB below the radiation peak, while the θ_g curve for 34.7 GHz (the high end of the Ka-band uplink) intersects partially with the $\theta_h = 14.0$ deg contour. This implies that there may be grating lobe effects at the high end of the Ka-band uplink. Since there is no noise consideration in the uplink band and only a slight power increase would be

required to compensate for the additional loss, this grating lobe problem is not considered to be severe.

IV. Conclusion

The design of an X-/Ka-band dichroic plate is presented. The theoretical calculations show excellent performance at the Ka-band downlink frequency and show a reflection loss that meets the requirement at the KABLE frequency. The analysis of the grating lobe effects predicts that there is no grating lobe problem at either the Ka-band downlink or KABLE frequencies, yet there may be grating lobe effects at the high end of the Ka-band uplink. This needs to be verified by experiments.

References

[1] J. C. Chen, "Analysis of a Thick Dichroic Plate with Rectangular Holes at Arbitrary Angle of Incidence," *TDA Progress Report 42-104*, vol. October–December 1990, Jet Propulsion Laboratory, Pasadena, California, pp. 9–16, February 15, 1991.

[2] R. E. Collin, *Foundations for Microwave Engineering*, New York: McGraw-Hill Physical and Quantum Electronics Series, p. 103, 1966.

Table 1. Tolerance study of hole size

Frequency, GHz	Polarization	Hole size, in.				
		$H_x = 0.200$ $H_y = 0.203$	$\Delta H_x = -0.001$	$\Delta H_x = +0.001$	$\Delta H_y = -0.001$	$\Delta H_y = +0.001$
		Reflection loss, dB	Δ Reflection loss, dB	Δ Reflection loss, dB	Δ Reflection loss, dB	Δ Reflection loss, dB
32.3 (Ka-band downlink)	TE	0.023	+0.002	+0.016	+0.003	−0.002
	TM	0.025	−0.001	+0.002	−0.015	+0.019
33.8 (KABLE)	TE	0.007	+0.003	−0.004	+0.000	−0.001
	TM	0.199	−0.005	+0.004	+0.001	−0.003
34.7 (Ka-band uplink)	TE	0.078	−0.017	+0.019	+0.002	−0.002
	TM	0.096	−0.002	+0.003	+0.009	−0.008

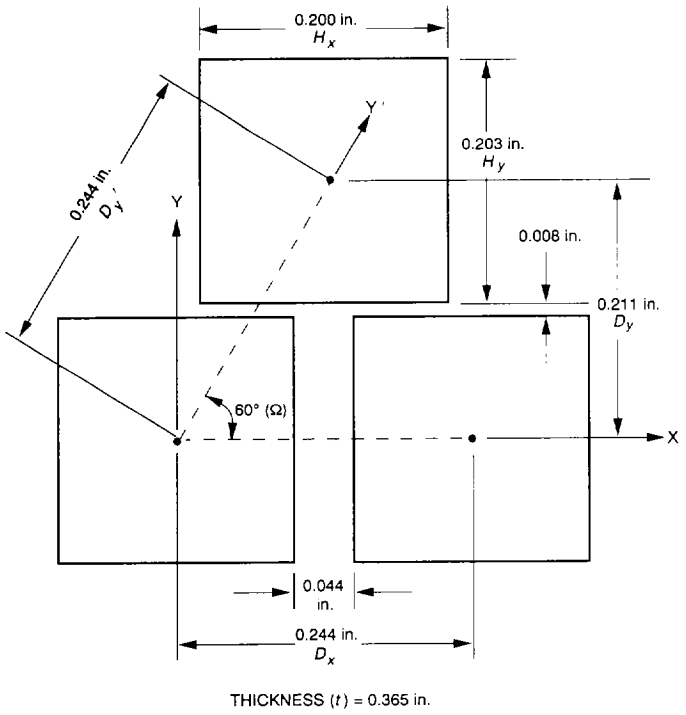

Fig. 1. Geometry of X-/Ka-band dichroic plate with rectangular holes.

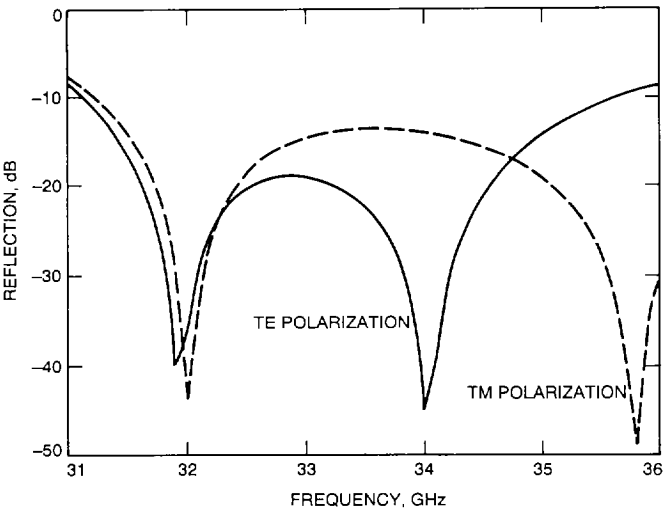

Fig. 3. Theoretical reflection versus frequency for X-/Ka-band dichroic plate for TE and TM polarization.

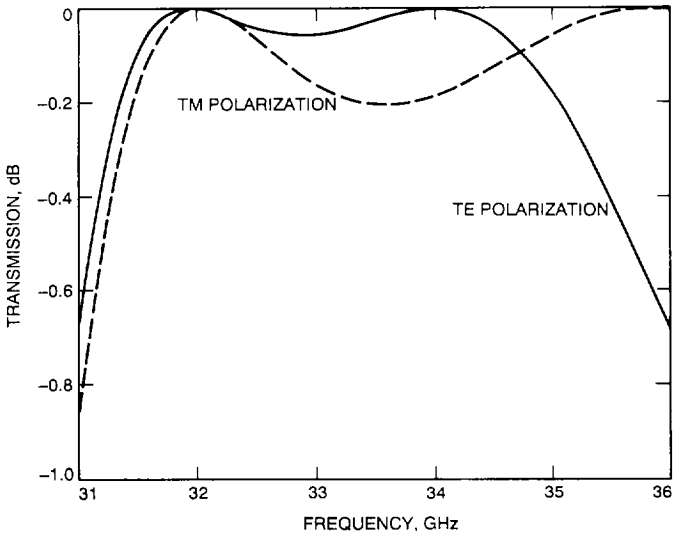

Fig. 2. Theoretical transmission versus frequency for X-/Ka-band dichroic plate for TE and TM polarization.

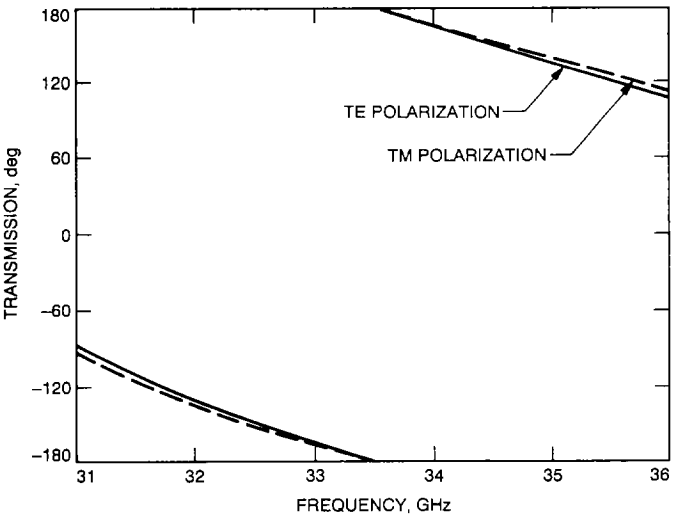

Fig. 4. Theoretical transmission phase versus frequency for X-/Ka-band dichroic plate for TE and TM polarization.

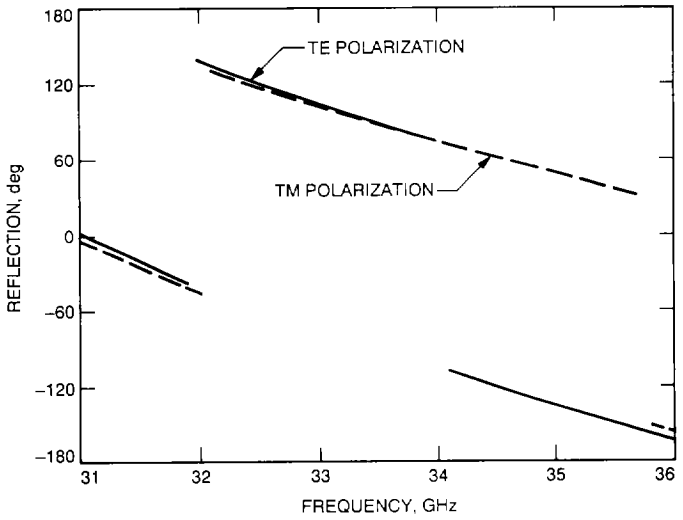

Fig. 5. Theoretical reflection phase versus frequency for X-/Ka-band dichroic plate for TE and TM polarization.

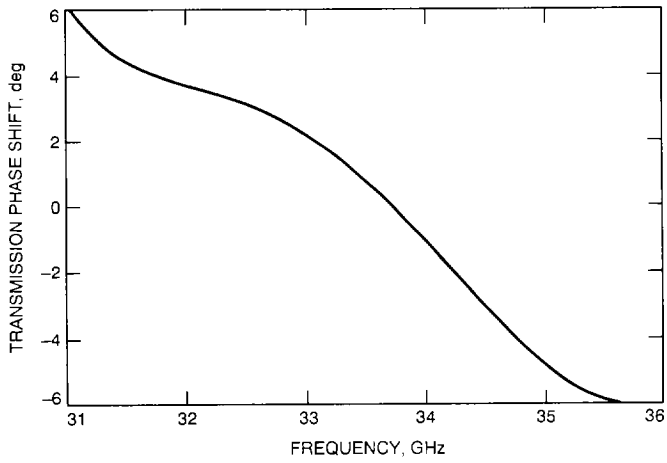

Fig. 6. Phase shift between TE and TM polarization versus frequency for X-/Ka-band dichroic plate.

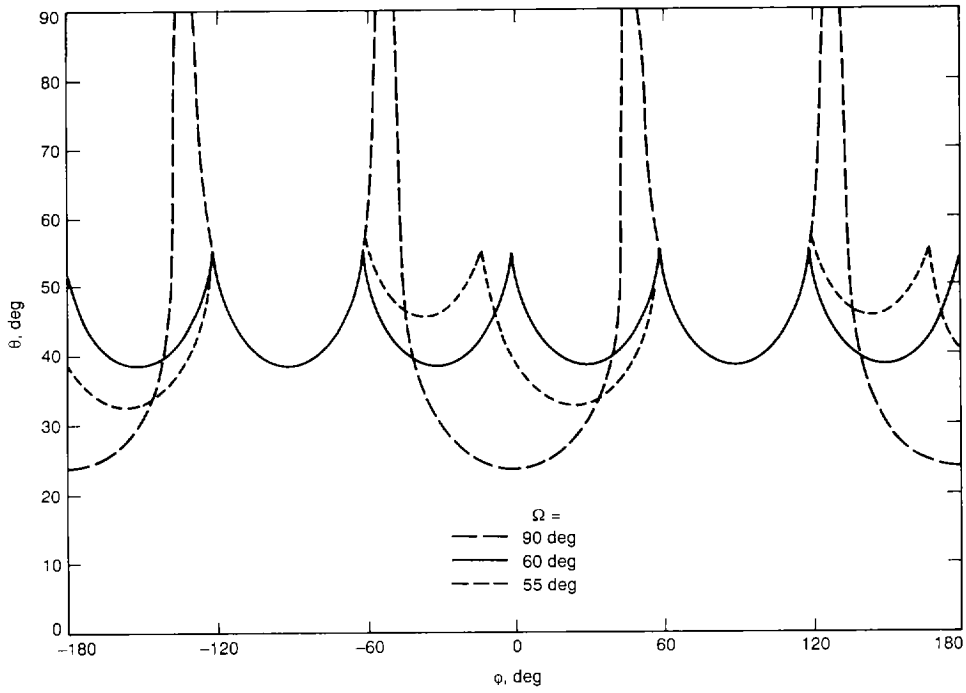

Fig. 7. Grating lobe curves for various skew angles (Ω) at a certain frequency (wavelength = 1.4 D) with cells of $D_x = D$, $D_y = 0.866D$, where D is a unit length.

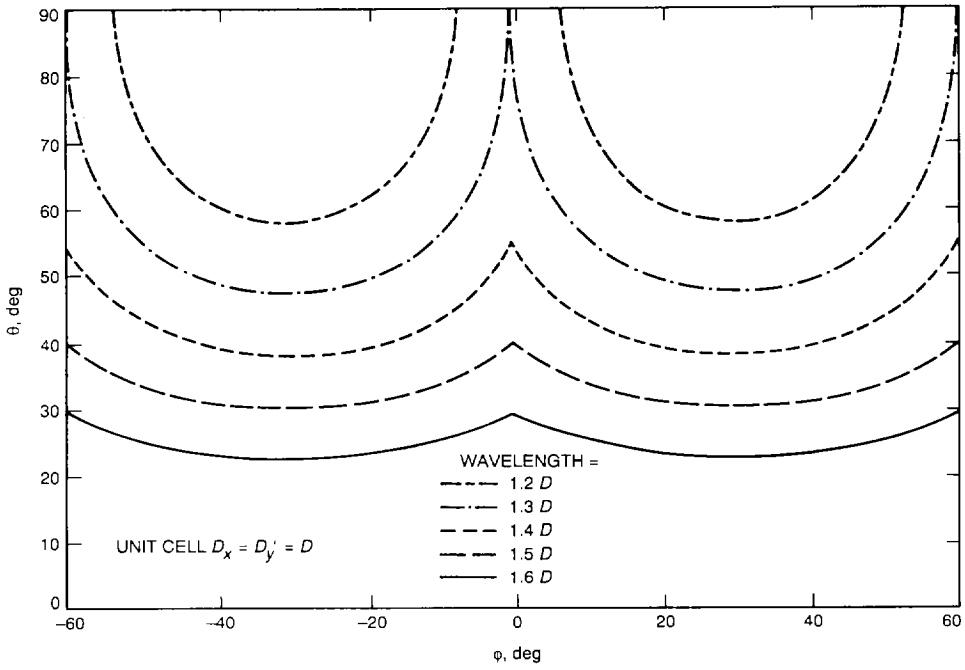

Fig. 8. Grating lobe curves for various frequencies (wavelength = 1.2 *D* to 1.6 *D*) with a cell of $D_x = D$, $D_y = 0.866D$, and $\Omega = 60.0$ deg, where *D* is a unit length.

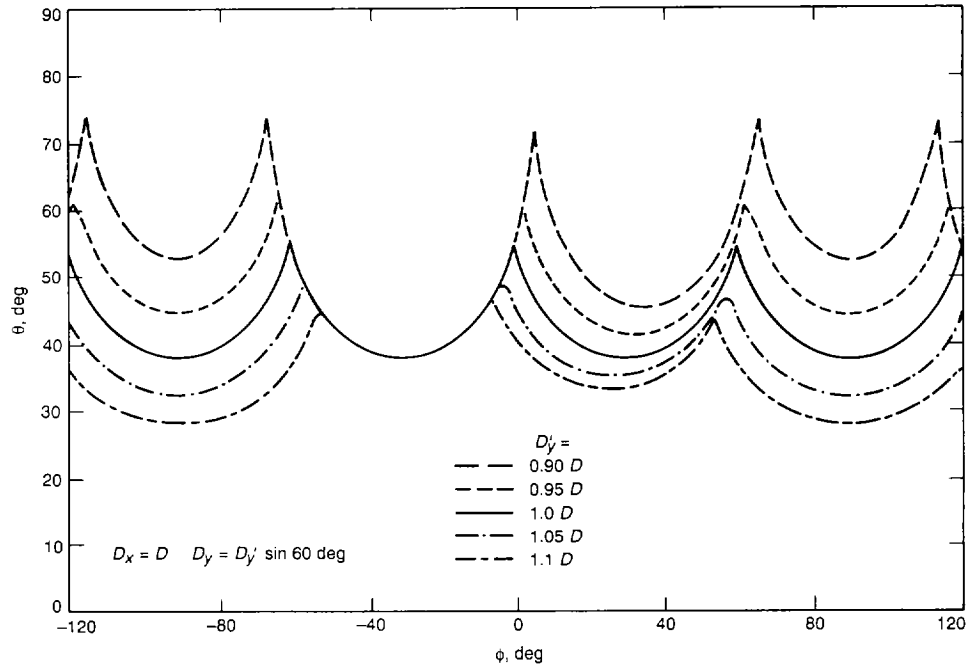

Fig. 9. Grating lobe curves with different Y′ components for a cell of $D_x = D$, $D_y' = D$, and $\Omega = 60.0$ deg, where *D* is a unit length.

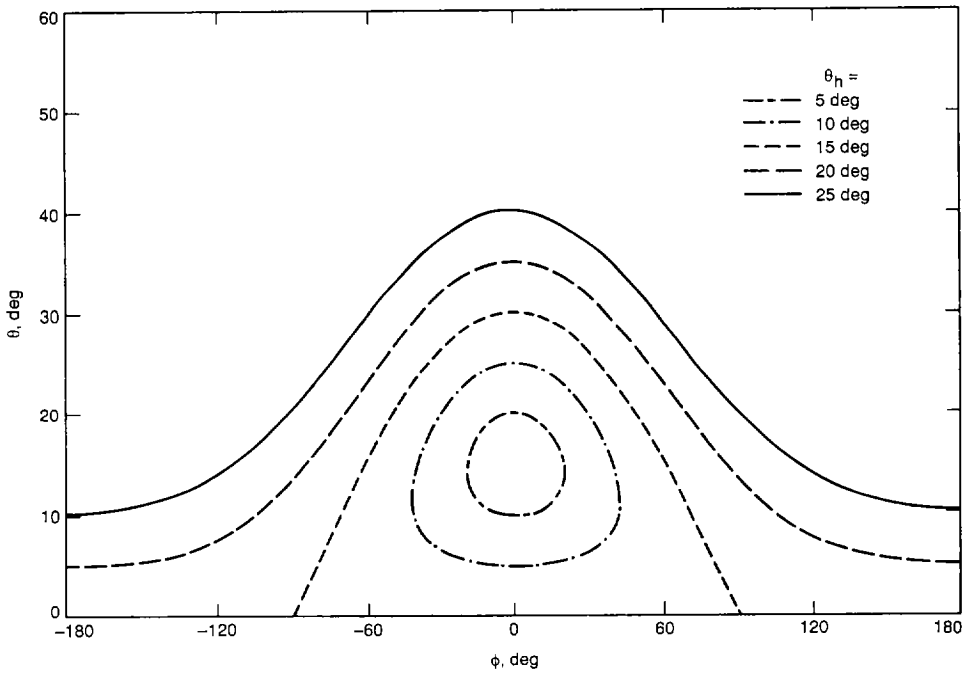

Fig. 10. Contour plot of horn pattern in terms of angles of incidence for a horn with principal angle at $\theta_0 = 15.0$ deg, $\phi_0 = 0.0$ deg.

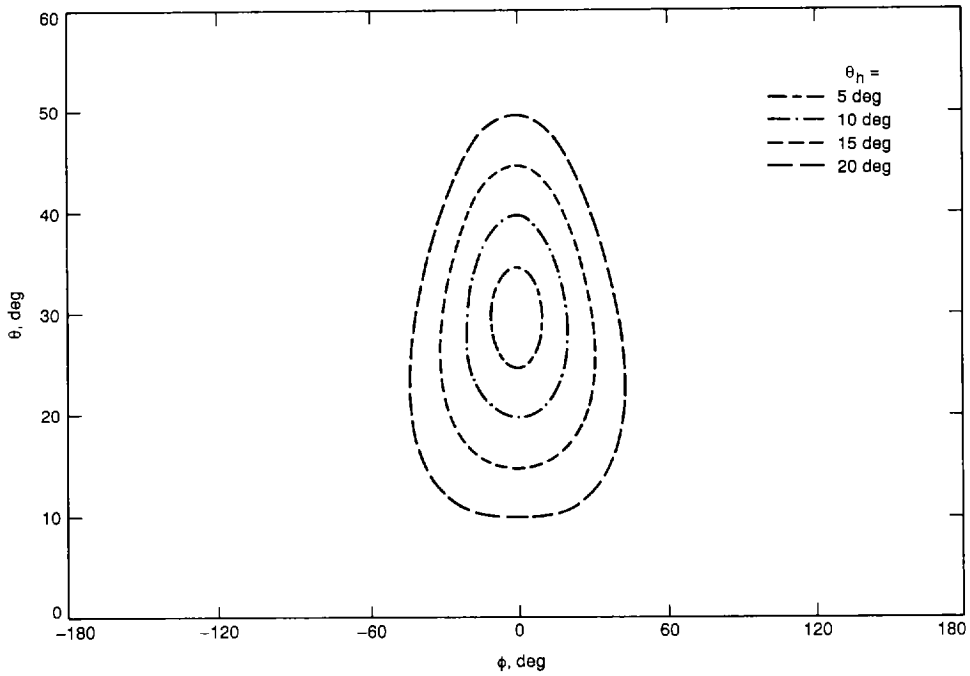

Fig. 11. Contour plot of horn pattern in terms of angles of incidence for a horn with principal angle at $\theta_0 = 30.0$ deg, $\phi_0 = 0.0$ deg.

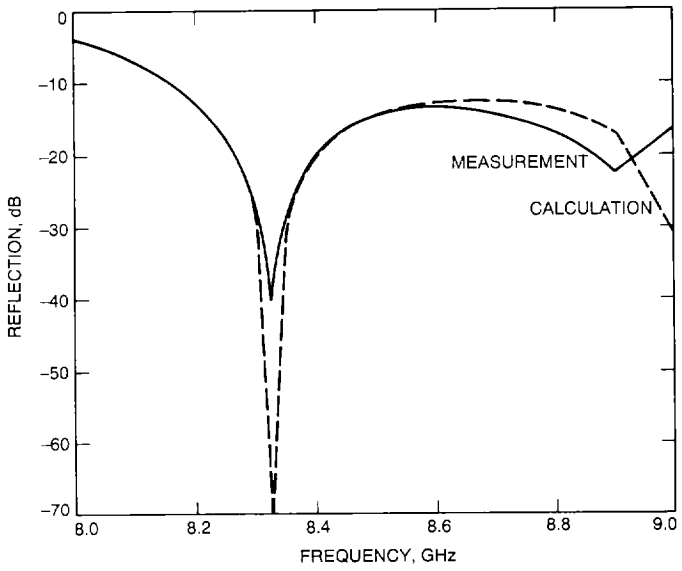

Fig. 12. Measured and calculated reflection versus frequency for the test S-/X-band dichroic plate.

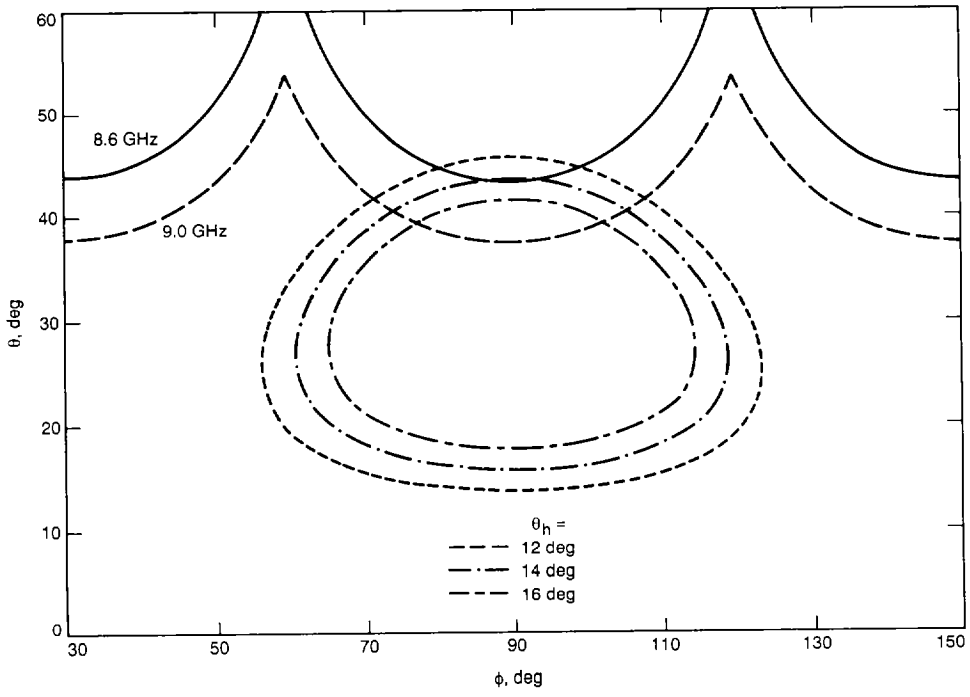

Fig. 13. Excitation of grating lobes by the feedhorn pattern for the test S-/X-band dichroic plate.

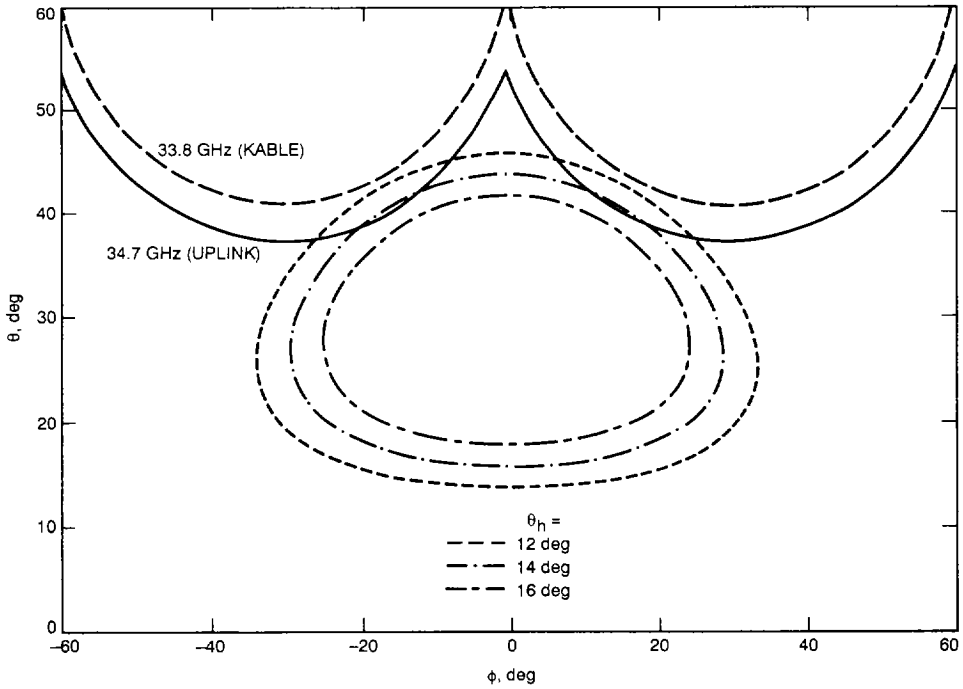

Fig. 14. Excitation of grating lobes by the feedhorn pattern for the X-/Ka-band dichroic plate.